

**Resolution Studies for a  
Multi-chromatic Time-of-Propagation Endcap DIRC for PANDA**

October 31, 2007

*M. Düren, M. Ehrenfried, S. Lu, R. Schmidt, P. Schönmeier*

*II. Physikalisches Institut  
Justus-Liebig-Universität Gießen  
Heinrich-Buff-Ring 16  
D-35392 Gießen*

**Abstract**

Resolution studies for the Time-of-Propagation Endcap DIRC design are presented. A new fitting method is introduced, which allows to separate pions and kaons using TOP measurements without knowing the time  $T_0$ , where the particle passed the detector. Calculations have been done for an updated geometry of the Giessen DIRC design with the result that pion - kaon separation up to 5 GeV/c is feasible at the  $4\sigma$ -level.

This report is located at  
<http://www.physik.uni-giessen.de/dueren/giessendirc2.pdf>

## Overview

During the last months, the conceptual design of the Giessen DIRC has been subject of intense studies and was subsequently refined in several respects compared to the original design described in [1]. One of the major modifications is changing the shape of the DIRC disk from an almost circular polygon to a polygon with a much lower number of corners (like six or eight as opposed to previously several hundred corners). It turned out that this geometrical shape helps resolving ambiguities in the observed photon hit pattern (see Fig. 1).

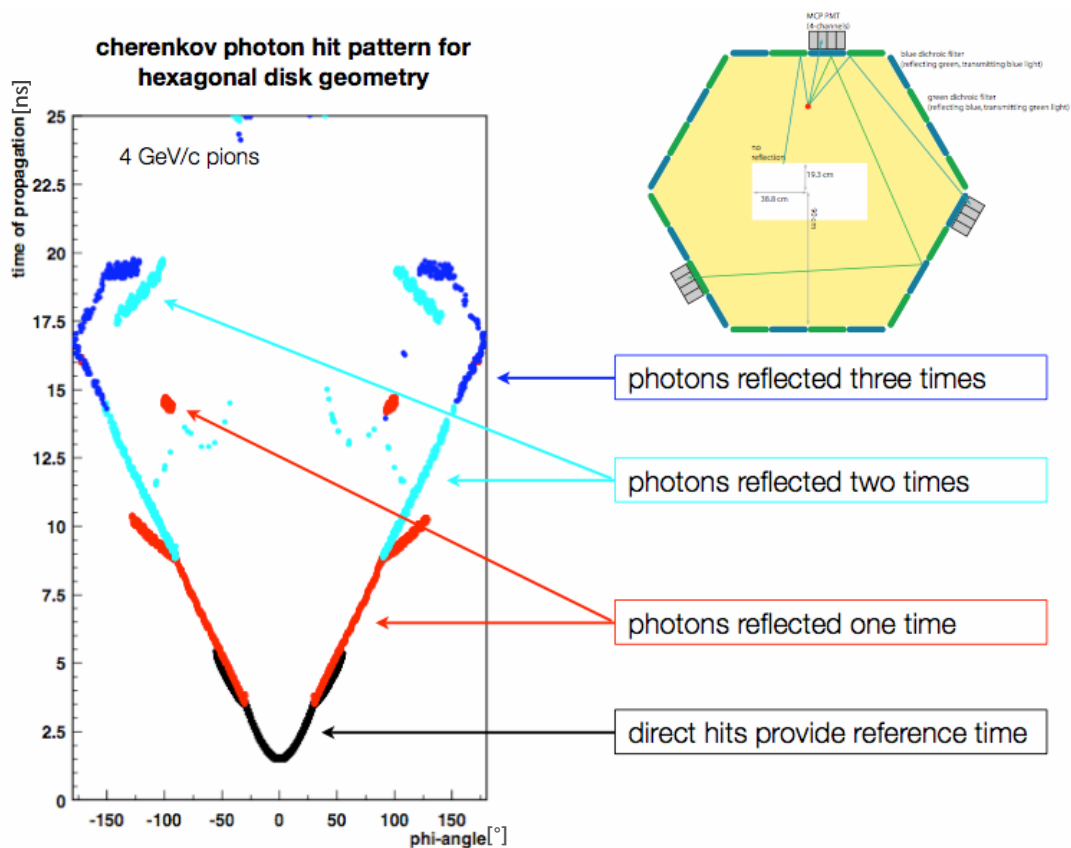


**Fig. 1:** Hit pattern of photons, observed in a DIRC disk with a low number of corners. If photons are detected in the vicinity of edges, the time of propagation of photons which are reflected  $n$  times and photons which are reflected  $(n+1)$  times is very similar. This causes ambiguities within the time resolution of the readout system. Therefore a low number of corners is advantageous as it increases the separation of different branches (like e.g. the black and the red branch belonging to zero and one reflection in the TOP range  $[2.7\text{ ns} \dots 5.0\text{ ns}]$  in the plot shown above).

Recent studies concentrate on the design of a smaller DIRC disk, which could be placed closer to the target (located inside the magnet instead of inside the magnet's return yoke). This to reduces as well the cost of the DIRC disk

(less material needed) as the cost of the detectors located downstream, in particular the Endcap ECAL [3]. It will be discussed more detailed later in this report.

### Factors of influence concerning the resolution

Based on the relatively high index of refraction for fused silica, the pion-kaon separation is easily feasible for low momenta up to 2.5 GeV/c. In the momentum range above 3.5 GeV/c separating kaons and pions usually becomes quite problematic as the opening angles of the Cherenkov cones converge towards the same saturation value (see Fig. 2).

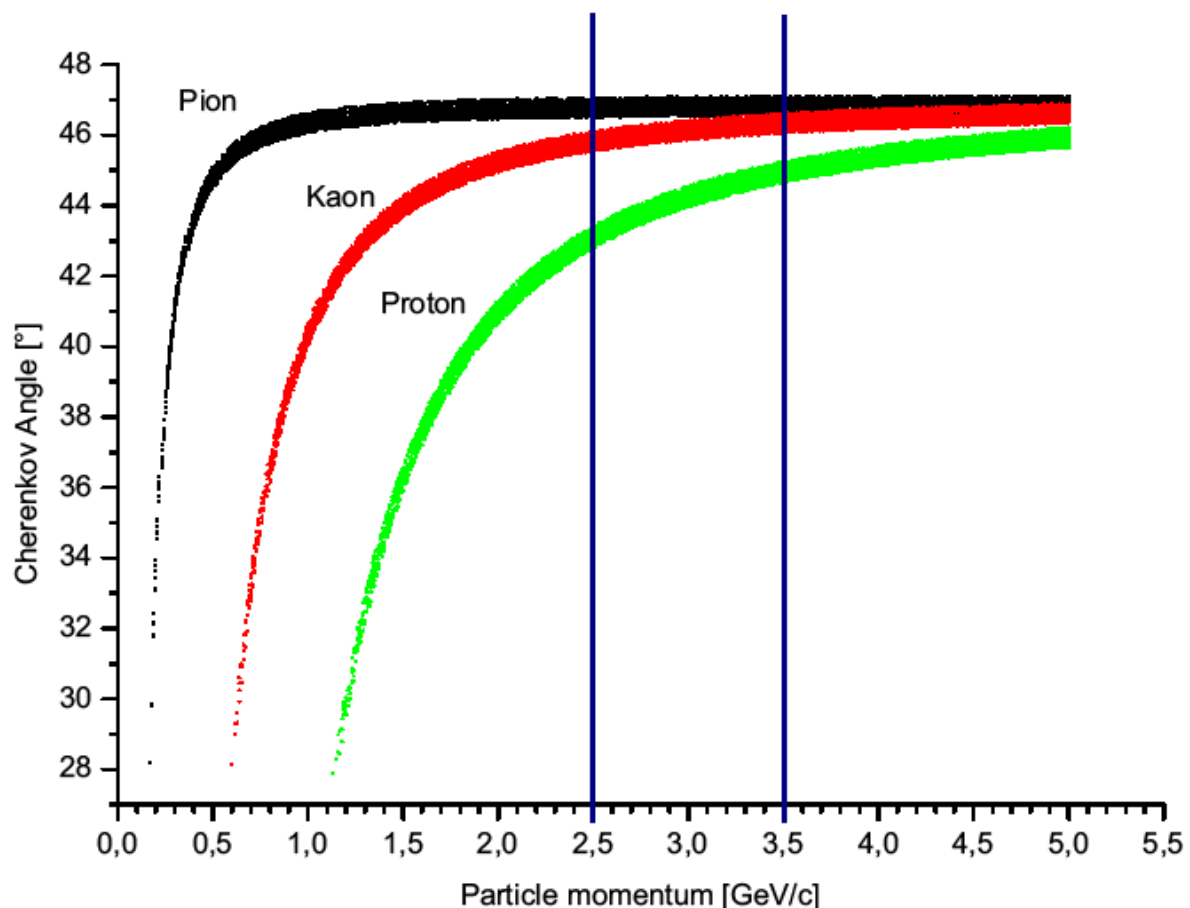


*Fig. 2:* Calculated Cherenkov angle as function of the wavelength. Wavelength is shown from 400 nm to 700 nm. Separation at 2.5 GeV/c and 3.5 GeV/c is indicated by vertical lines.

The following table describes the main effects influencing the quality of the final Cherenkov detector:

Effect	Impact	Simulation
<b>Dispersion</b> caused by change of refractive index $n(\lambda)$	Dispersion widens distributions as photons travel at different group velocities through the material and as the Cherenkov angle depends on the index of refraction. It can be reduced by restricting the accepted spectral range or some sort of dispersion correction (e.g. dichroic mirrors).	Refractive index parameterized; fully simulated for every single photon during ray tracing.
<b>Reflective properties</b> of dichroic mirrors	Reflective properties of dichroic mirrors change depending of incident angle of photons.	Parameterised in Monte Carlo based on measurements with sample mirrors.
<b>Time resolution</b> of readout system	Crucial quantity for a TOP DIRC, depending e.g. on $\sigma_{TTS}$ of the PMT and time resolution of TDC. ( $\sigma_{TTS}$ is the transition time spread specific for the PMT)	Time binning / smearing of 50 ps implemented in Monte Carlo.
<b>Angular resolution</b> of photon readout (pixel size)	Determines resolution of $\varphi$ coordinate (angle measured along the circumference of the disk)	Implemented; currently 960 detector pixels around the disk, for the reconstruction the centre position of each detector is used.
<b>Thickness of radiator</b>	Thicker radiator increases path length of particles: ⇒ higher photon statistics (good!) ⇒ increased uncertainty on emission point of photons  also: <b>multiple scattering</b>	Implemented in simulation.  (not yet implemented)

Effect	Impact	Simulation
<b>Surface quality</b> of radiator	Surface roughness causes angular straggling and therefore smearing on the reconstructed Cherenkov angle.	Not yet implemented. Measurements needed to parameterise this effect.
<b>Light attenuation</b> inside the radiator	Reduces photon statistics, hence increasing the spread of measured values.	Coarsely implemented in simulation as there are currently no measurements available which could be parameterised.
<b>Quantum efficiency</b> of photon detectors	Reduces photon statistics, hence increasing the spread of measured values.	Impact of different quantum efficiencies has been studied.
<b>Angle of incidence</b> of the particles	Particles entering the radiator under shallow angles will produce a higher photon yield, which comes at the cost of a higher uncertainty on the emission point of the photons.	Completely simulated; Optimization problem coupled to choice of optimum radiator thickness as the angular acceptance of $10^\circ$ - $22^\circ$ is a given quantity.
<b>Central aperture</b> for forward spectrometer acceptance: $\pm 10^\circ$ horizontally $\pm 5^\circ$ vertically	Is absorbing in the current design. Is possibly set to be reflecting for special test.	Absorbing hole is completely simulated. Test with a reflecting hole are done.
<b>Uncertainties of initial track parameters</b> (position, angle and momentum of the particle)	Additional smearing	Not yet implemented

## Detector geometry

The technical boundary conditions require that the Endcap DIRC has to cover the acceptance from  $5^\circ$  to  $22^\circ$  in vertical direction and from  $10^\circ$  to  $22^\circ$  in horizontal direction. In the following paragraphs we introduce two possible scenarios for the position of the DIRC (see Fig. 3)

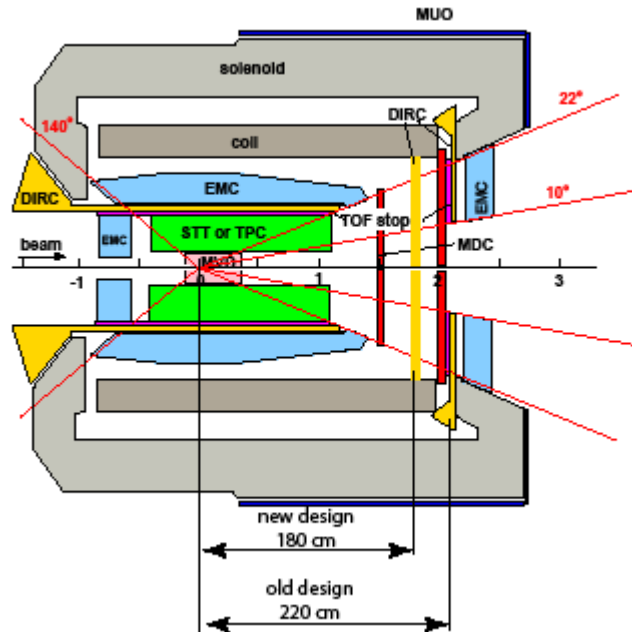


*Fig. 3:* Side view of the central part of the Panda detector. Two possible positions for the Disk DIRC are shown (vertical yellow bars). The old design, described in chapter “Scenario A” is located 220 cm downstream the IP point. The new design, described as Scenario B, is located 180 cm downstream the IP point. The covered acceptance range is  $5^\circ$  to  $22^\circ$  horizontally and  $10^\circ$  to  $22^\circ$  vertically.

### Scenario A: “large disk”

In our original conceptual design report [1] we studied the scenario placing the Endcap DIRC at a distance of 2.2 m downstream the interaction point (IP), inside the return yoke of the target spectrometer’s solenoid magnet. At this position the strength of the magnetic field might reach values of about 1.5 T, which are easily withstood by MCP PMTs.

In this scenario the radiator disk is of hexagonal shape and has a thickness of 2 cm. Each side of the hexagon is equipped with 160 pixels, resulting in 960 readout channels in total. The photon readout is sensitive only to visible light in the range 400nm – 700 nm and the dichroic mirrors in front of the PMT pixels alternate channel by channel (contrary to the sketch shown in Fig. 4 where they alternate in groups of four pixels)

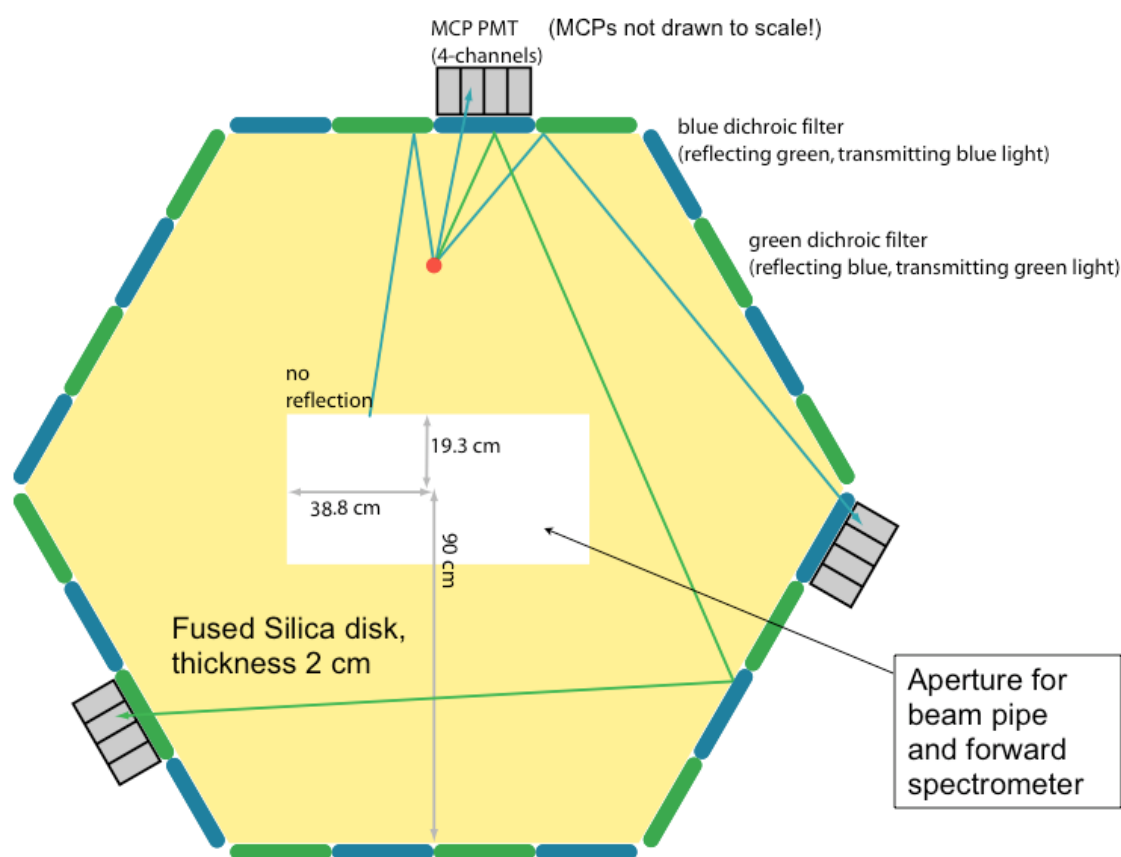


**Fig. 4:** Scenario A: “large disk”. In this version a hexagonal disk with a readout of 960 MCP PMT channels is located 2.2 m downstream of the IP. Please note that in the simulation the colour of the dichroic mirrors alternates pixel by pixel instead of in groups of four pixels as shown in the sketch.

### Scenario B: “small disk”

As suggested recently [3], we simulated also the option of placing the Endcap DIRC much closer to the target at a distance of 1.8 m downstream of the IP, inside the magnet itself. At this position free space of up to 94 cm radial from the beam axis is available. According to the magnet's geometry an octagonal shape for the radiator disk seems to be the natural choice (Fig. 5). The magnetic field will reach values up to 2.4 T and it is not yet clear, which kind of photon detectors will be proposed for use under such conditions.

The other design parameters are identical to Scenario A; each side of the radiator disk is equipped with 120 MCP PMT pixels, resulting in the same total number of 960 pixels and thus in the same angular resolution. The colour of the dichroic mirrors alternates from pixel to pixel.

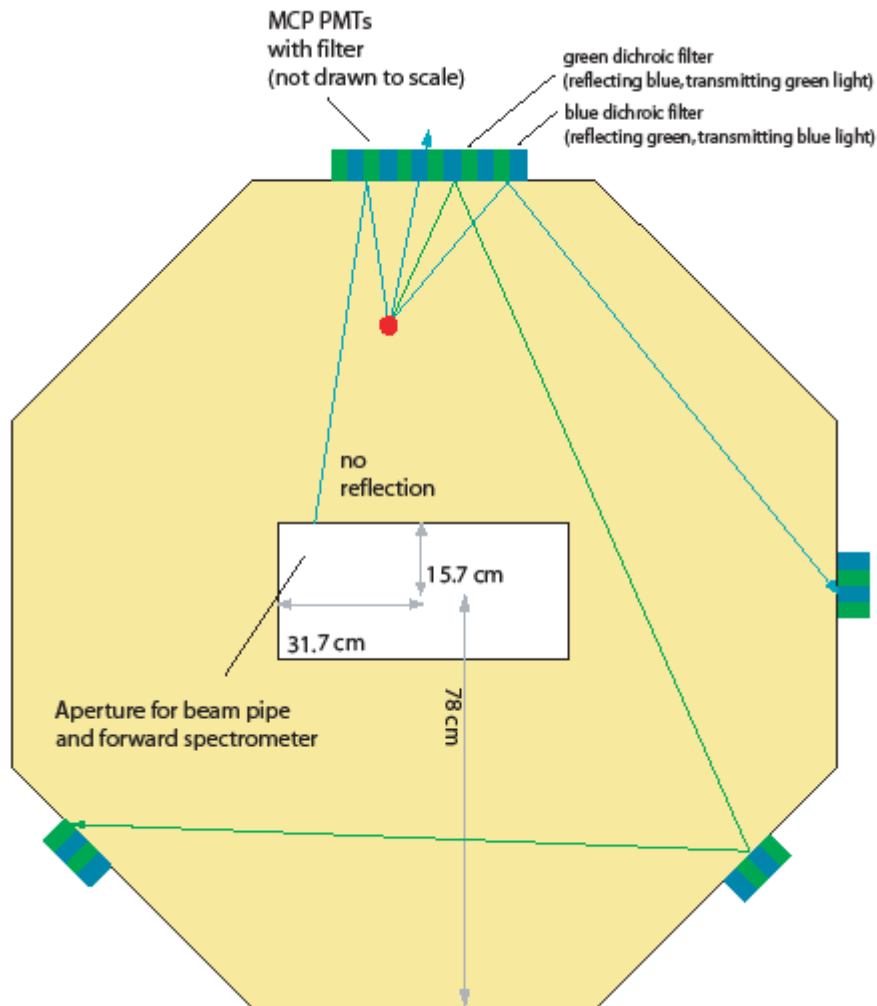


**Fig. 5:** Scenario B: “small disk”. The octagonal disk (thickness: 2 cm) with a readout of 960 MCP PMT pixels is located 1.8 m downstream of the IP.

### **Scenario B+GEM: “small disk with additional GEM readout”**

As an alternative design, it was suggested to use a liquid radiator proximity focusing RICH detector with GEM readout [3]. The advantage of GEM detectors would be that they additionally provide tracking information as also the charged particle produces a hit which is due to its signal height clearly distinguishable from the hits produced by Cherenkov photons.

We plan to study if the fused silica Disk DIRC can be used as radiator as well for the internally reflected light, as also at the same time for a GEM that detects the rings of the non-reflected Cherenkov photons. For the B+GEM Scenario we placed 10 cm downstream the DIRC radiator (i.e.: IP at  $z=0$  cm, DIRC radiator disk at  $z=180-182$  cm, GEM plane at  $z=192$  cm) a GEM plane to detect those Cherenkov photons, which exit the radiator at the back side. If a charged particle traverses the radiator, a certain fraction of the photons (depending on the angle of incidence) will be internally reflected. The rest of the photons will exit the disk.

It may turn out that combining a DIRC with an additional GEM readout will increase the redundancy of information and therefore improve PID capabilities.

### **Dichroic Mirrors**

Chromatic correction is achieved by using dichroic mirrors/filters that are placed in front of the photon detectors. In our current simulation there are two different types of mirrors placed in front of the PMT pixels, alternating pixel-by-pixel, splitting the spectral range of Cherenkov photons at 500 nm: “green” filters transmit “green” photons in the range [500 ... 700 nm] and reflect “blue” photons in the range [400 ... 500 nm]. Accordingly “blue” filters are optimised vice versa.

The application of dichroic mirrors is of twofold advantage: Firstly it allows assigning an appropriate index of refraction during the reconstruction process as the approximate wavelength of the detected photon is known within the transmission band of the dichroic filter placed in front of the photon detector. Secondly the reflections arising for photons that have the ‘wrong’ colour to pass the filter prolong the path length within the material. Although this comes at the cost of reduced photon statistics due to absorption, these photons carry a large content of information as the TOP difference between photons emitted under different Cherenkov angles increases linearly with the path length. This leads to larger (and therefore easier measurable) time differences (Fig. 6).

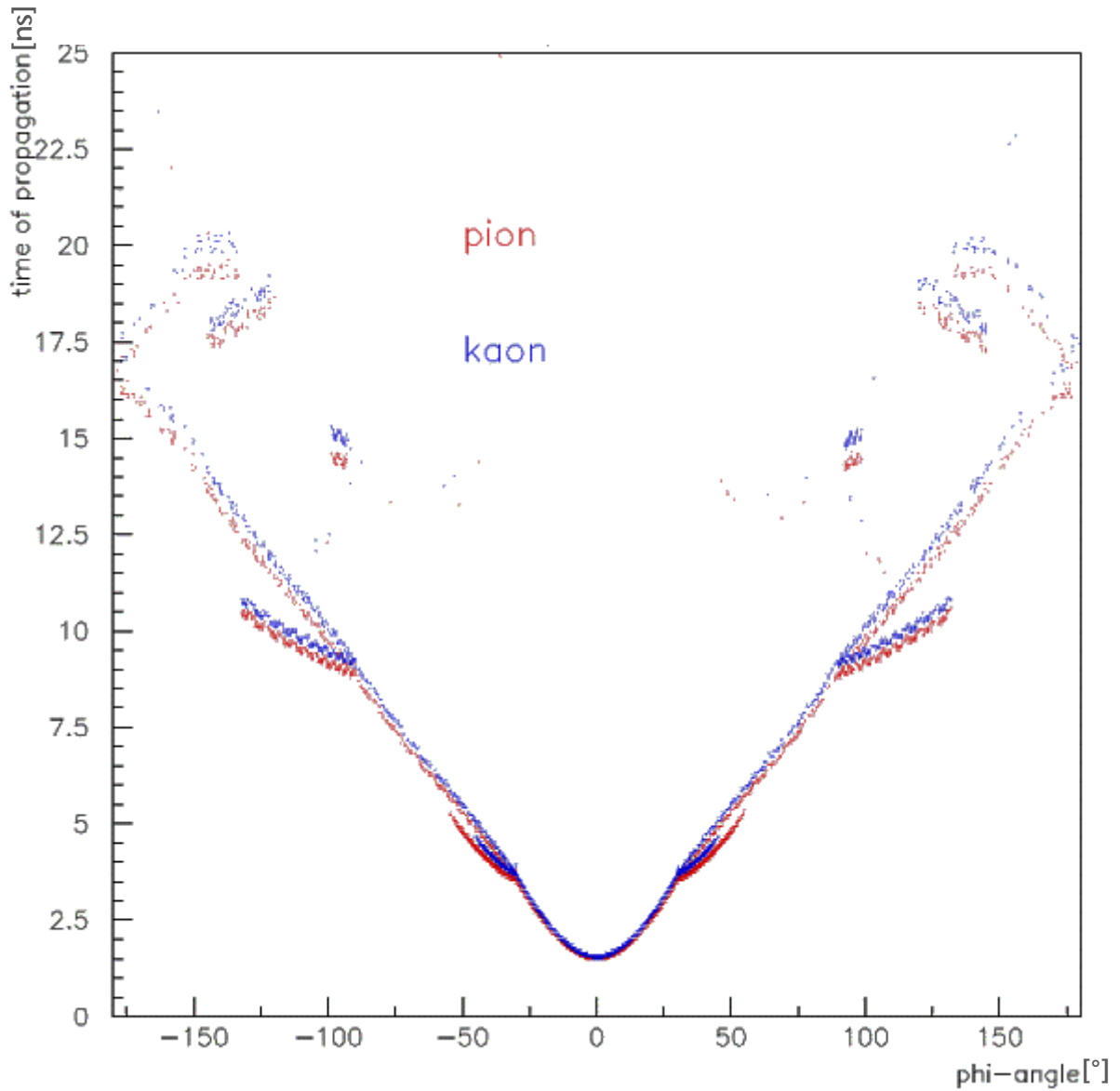


**Fig. 6:** Time of propagation (TOP) versus azimuthal angle  $\phi$  for the Cherenkov photons from 50 pions (red) and kaons (blue). The angle  $\phi$  is the azimuthal angle with respect to the detector centre for a pion or kaon that crosses the disk at 12 o'clock with an inclination that points vertically. The diagram shows the result of the simulation of 1.5 GeV particles. The separation of the pion and kaon signals for large values of TOP is clearly visible.

To some extent, the properties of dichroic mirrors depend on the angle of incident, as the reflection is achieved by interference effects. Obviously, for pure geometrical reasons, photons arriving under flat angles of incident are confronted with larger effective layer thicknesses than photons arriving under steep angles (Fig. 7). Fortunately, the optimization of dichroic mirrors to different angles of incidence is easily possible and custom-made mirrors are comparably cheap. The behaviour shown in Fig. 7 has been parameterised as a function of incident angle, fully implemented in our Monte Carlo and is therefore considered for all plots presented in this report.

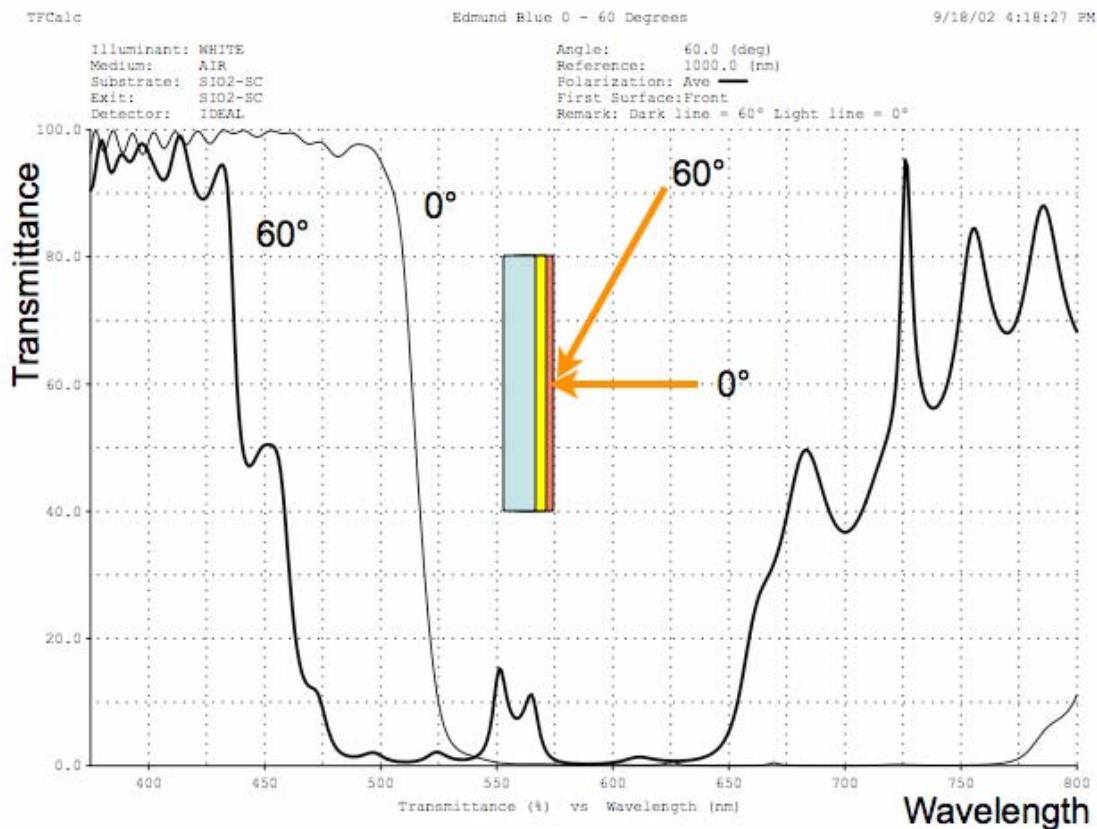


*Fig. 7: Transmittance of a dichroic mirror optimized for an incident angle of 0°. The sharp edge around 500 nm shifts towards lower values for more shallow angles of incidence.*

### Spatial and time resolution

The spatial resolution in azimuthal angle around the circumference of the DIRC disk is given by the number of PMT pixels. A total number of 960 pixels results in an angular resolution of approx.  $0.375^\circ$  (making the somewhat crude assumption of treating a hexagon or octagon as a circle and therefore neglecting the fact that the resolution near the corners is slightly different). In our studies the centre position of the photon detector pixels is used for reconstruction, taking the effects of spatial resolution into account.

The photon detector and its attached electronics determine the resolution in the TOP coordinate. A resolution in the order of 50 ps seems to be reasonably achievable. Smearing the true TOP value randomly by  $\pm 25$  ps and subsequently re-binning the values were the two steps used to simulate the effects of time resolution.

As shown in Fig. 8 the patterns produced by two different particles are clearly distinct with very small regions of ambiguity. Please note that the combined

resolution corresponds to approx. 400.000 pixels in the 2-dimensional TOP- $\phi$  - plane.

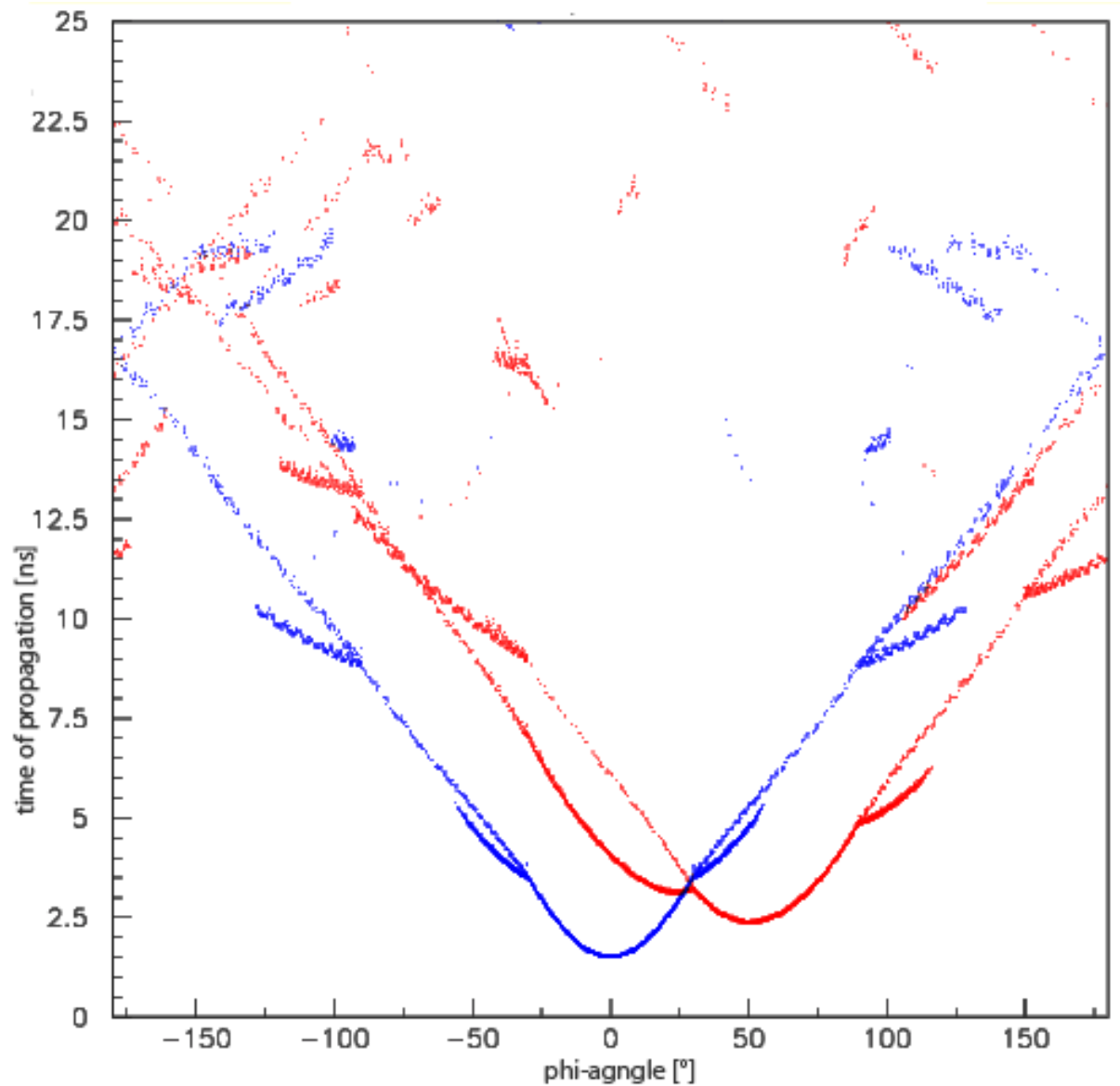


**Fig. 8:** TOP vs.  $\phi$  photon hit pattern of an event with multiple 4 GeV/c particles hitting the DIRC under two different angles and positions. The blue points belong to a particle hitting the disk under a scattering angle  $\theta=15^\circ$  at  $\phi=0^\circ$ , the red points are produced by a particle with the parameters  $\theta=12^\circ$  and  $\phi=44^\circ$ . Each particle produces 1-dimensional structures in a 2-dimensional plane and only very few points at the intersections become ambiguous.

### Comparison between Scenario A and B

The kaon / pion separation was studied as a function of momentum (Fig. 9).

The separation power  $N_\sigma$  is defined here as  $N_\sigma = \frac{|Mean_1 - Mean_2|}{\sqrt{\sigma_1^2 + \sigma_2^2}}$ , which is dif-

ferent to the definition at the end of the report (see page 17). Within uncertainty, no significant difference was observed for the kaon/pion separation power of Scenario A and B. The ratio between the values displayed in the plots of Fig. 9 is compatible with unity as shown in Fig. 10 (with a slight advantage for the smaller disk at low particle momentum where the separation is anyway very good).

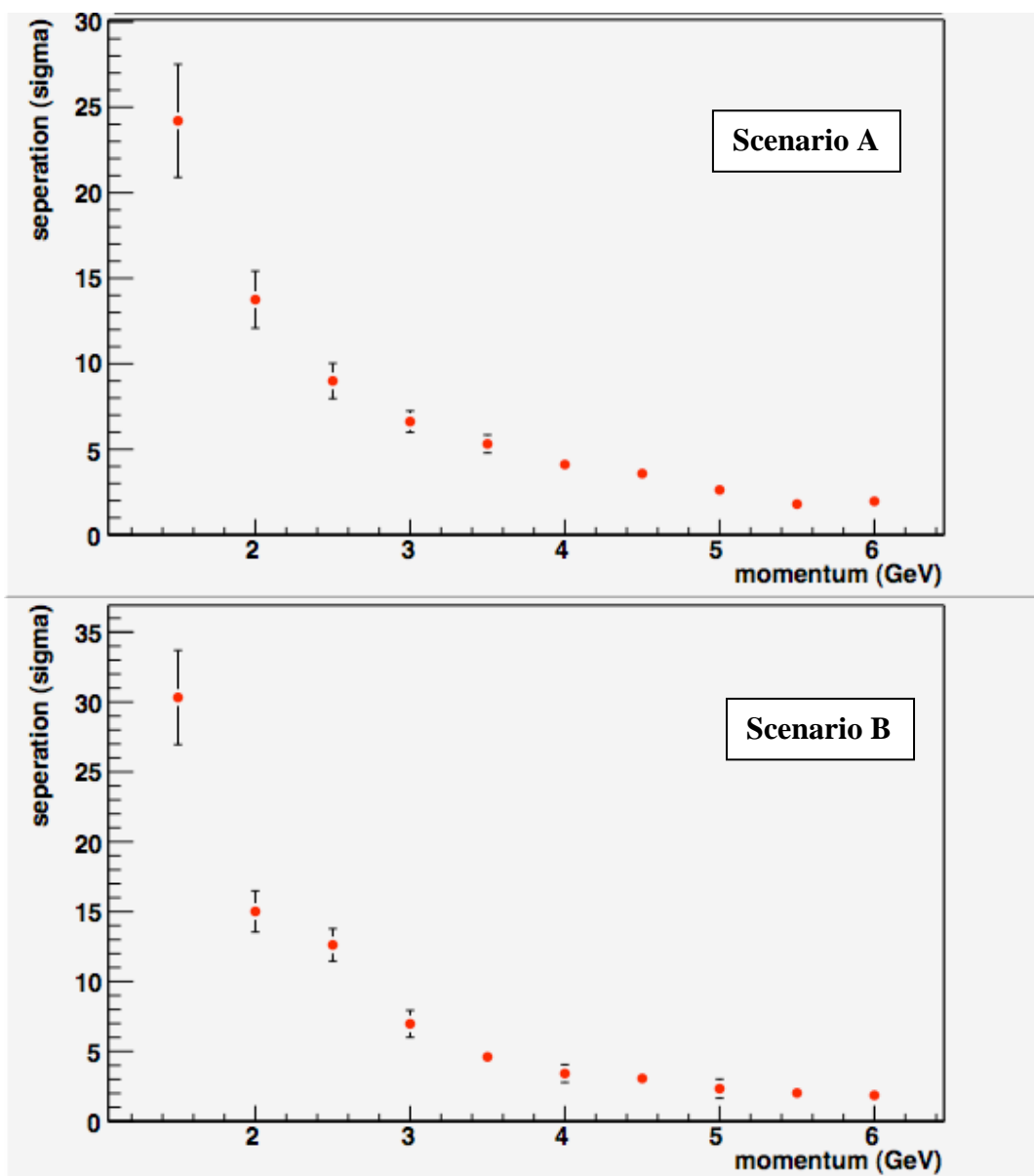
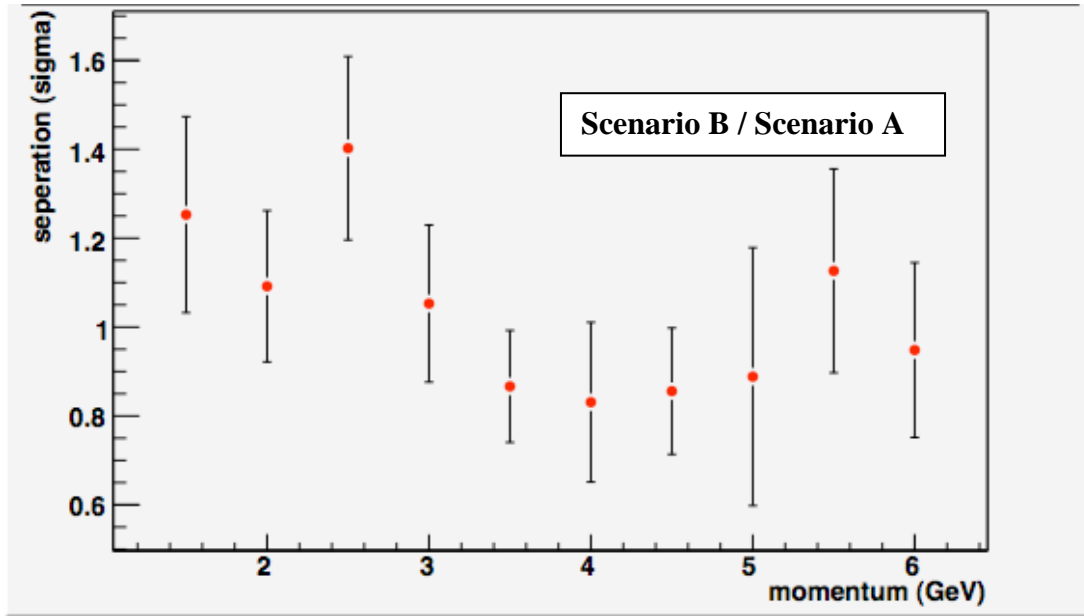


Fig. 9: Kaon / pion separation as a function of the particle's momentum.



*Fig. 10: Ratio of momentum dependent kaon / pion separation depicted in Fig. 9. Within uncertainty both scenarios deliver a very similar performance with a slight advantage for the smaller radiator disk in the low momentum region.*

### Slope-Fitting Method

In the previous chapter, we compared the large disk (hexagon, 220cm from IP) with the small disk (octagon, 180cm from IP). Both results were gained by analytically calculating the Cherenkov angle using the ToP. This method works fine as long as the time  $T_0$  where the particle crosses the DIRC is exactly known in the experiment. If  $T_0$  is smeared out, the separation power decreases seriously.

To avoid this problem we developed a  $T_0$  independent method to separate pions and kaons. In the following paragraphs it is explained how this new method works. All the results of this new method are calculated from the dataset of the Monte Carlo for the “small” disk as described before.

It is assumed that the relative timing of all photon detectors is synchronized, while the time of incident of the particle is completely unknown. The fitting method is based on the fact that a particle emits several photons with different path length, which arrive at different times at the detectors and that these (projections of the) path lengths are known. The measured parameters (angles, positions etc.) are used to calculate the ToP and to compare it with the ToP measured in the experiment. With  $T_0$  as a free parameter, a pion-hypothesis and a kaon-hypothesis can be tested separately. The hypothesis where the calculated and the measured TOP values agree better indicates

the true particle type. All “measured” values are gained by the Monte Carlo simulation. The calculated ToP is based on the following variables:

- $P$ , this is the momentum of the particle. This parameter is not smeared.
- The position of the point where the photon is emitted from the particle. This parameter is smeared.
- $\Theta$ , this is the entrance angle of the particle when hitting the disk. This parameter is not smeared.
- $\Phi$ , this is the direction of the photon emitted from the particle. This parameter is smeared.
- The position of the detector where the photon is detected. This parameter is smeared.
- The color of the mirror in front of the detector that was hit. The wavelength of the transition edge of the mirror is smeared. The reconstructed wavelength is set to 450 nm for all photons below 500 nm and set to 550 nm for all photons above 500 nm.

Additionally, the type of the particle is needed, but unknown. To handle this issue, the calculation is done with both hypothesis (pion and kaon). In order to gain advantage from the different colors of the mirrors in front of the detectors, calculations are done separately for wavelengths below and above 500 nm for each particle.

With that information four scenarios (two particle types with 2 color ranges each) are available for calculation of the ToP. Those scenarios are:

1. Assuming the particle to be a pion and only taking photons below 500 nm into account.
2. Assuming the particle to be a pion and only taking photons above 500 nm into account.
3. Assuming the particle to be a kaon and only taking photons below 500 nm into account.
4. Assuming the particle to be a kaon and only taking photons above 500 nm into account.

The ratio between those calculated ToP values and the measured ToP, from the Monte Carlo, returns a certain slope for each scenario. As example, two of them are shown in Fig. 11.

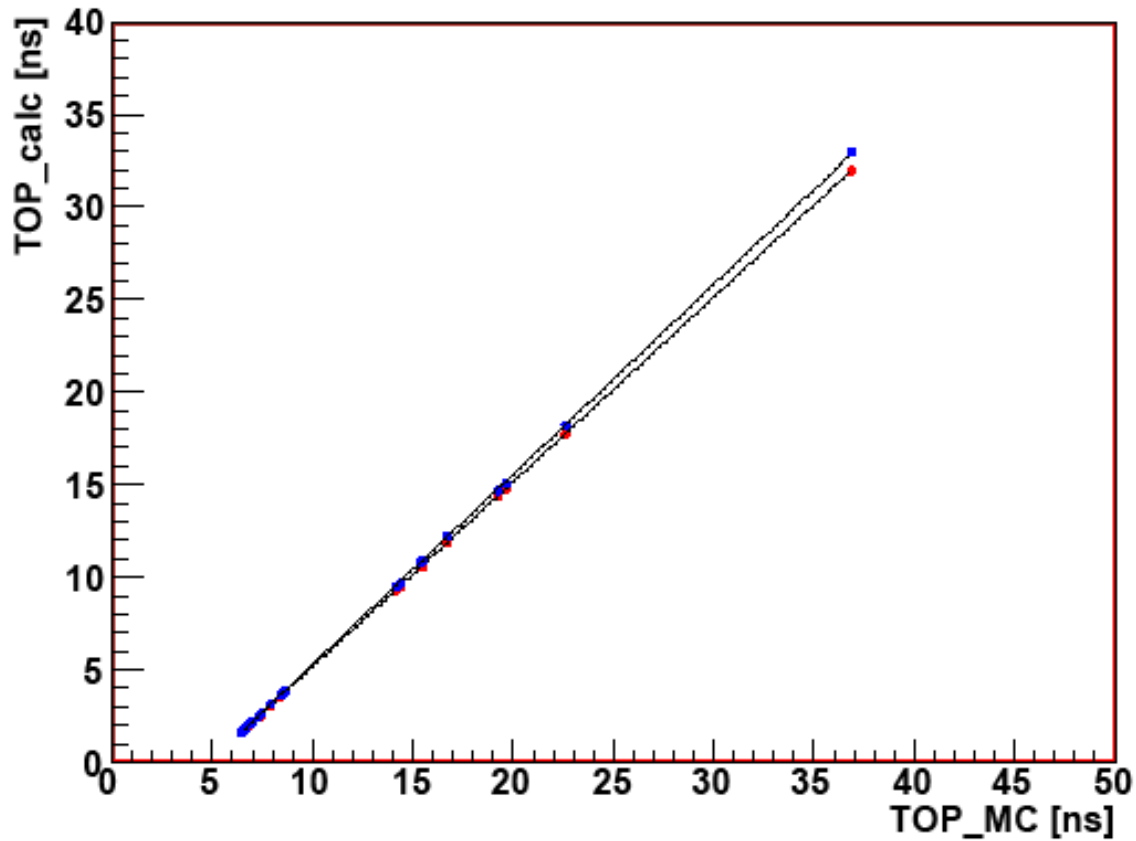


*Fig. 11* An example of linear fitting for a particle with a momentum of 2.0 GeV/c. The wave length of Cherenkov photons taken into account are from 500 nm to 700 nm. In this plots, 550 nm is used for the calculation of "TOP\_calc" based on two hypotheses. The blue point shows the calculation of "TOP\_calc" vs. ToP\_MC based on the hypothesis that the particle is a kaon. The red points are based on the hypothesis of pion. The two slopes have been acquired from fitting.

These slopes are called  $S_0$ ,  $S_1$ ,  $S_2$ ,  $S_3$ . By multiplying all those four slopes, characteristic value ( $X$ ) is found.

$$X = S_0 * S_1 * S_2 * S_3$$

The value  $X$  is used to decide for each event if it corresponds to a pion or kaon. The distribution in  $X$  has been extracted from Monte Carlo generating 500 pions and 500 kaons as shown in Fig. 12.

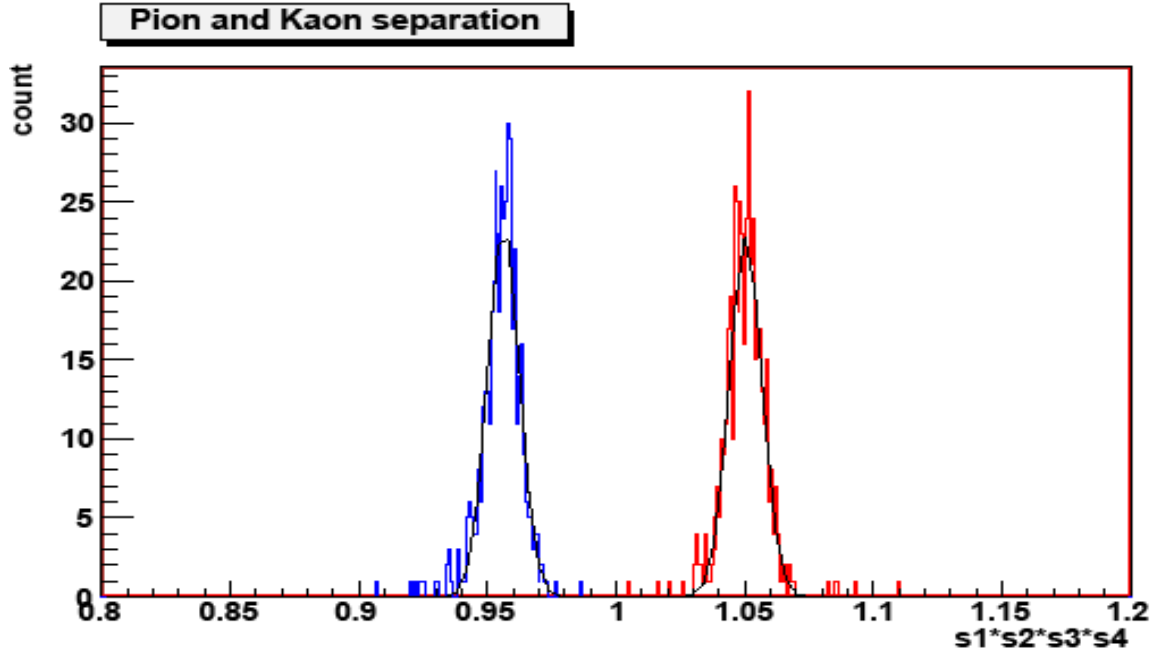


*Fig. 12* Separation of pions (red curve) and kaons (blue curve) using the characteristic value “X”. The black curves are the Gaussian fits. Two mean values and two  $\sigma$  values are extracted from this Gaussian fits, which are used to calculate the separation  $\sigma$ .

Though the actual particle is unknown, Fig. 10 shows that the method allows a good particle identification by cutting in  $X$  at  $X = 1$ . In case a pion was simulated, the value  $X$  is larger than 1. A simulated kaon results in a value  $X$  smaller than 1.

With the distribution shown in Fig. 12 and by applying Gaussian fits (also shown in Fig. 12) the separation power of the PID method was extracted for those two particle types. The separation  $N_\sigma$  in units of the average width  $(\sigma_1 + \sigma_2)/2$  of the two Gauss curves for pions and kaons is given by:

$$N_\sigma = \frac{|Mean_1 - Mean_2|}{\frac{\sigma_1 + \sigma_2}{2}} \quad (\text{red points in Fig. 13}).$$

$Mean_1$  is the mean value of the Gaussian fit for pions,  $Mean_2$  is the corresponding value for kaons. The values  $\sigma_1$  and  $\sigma_2$  are the standard deviation values of the Gaussian fits. This definition of the separation power is different to the one used before in this report (on page 13) and follows a recent decision in the PANDA group to have comparable definitions for bench mark numbers. Based on these calculations, a plot of the  $N_\sigma$  separation vs. the momentum of the particle is extracted as shown in Fig. 13.

For the symmetric case of two equal particle fluxes and widths for pions and kaons, a separation of  $4\sigma$  according to the above definition corresponds to a pion-kaon misidentification of 2.3%.

For comparison, Fig. 13 also includes a calculation according to a different definition of the separation power:

$$N_{\sigma}^{\text{conserv.}} = \frac{|Mean_1 - Mean_2|}{\sigma_1 + \sigma_2} \quad (\text{blue points in Fig. 13}).$$

In this “conservative” definition, a misidentification of 2.3% corresponds to a  $2\sigma$ -separation (and not  $4\sigma$ ); a  $3\sigma$ -separation corresponds to a misidentification less than 2 per mille. The conservative definition corresponds to the usual sigma separations as known from e.g. statistical error distributions.

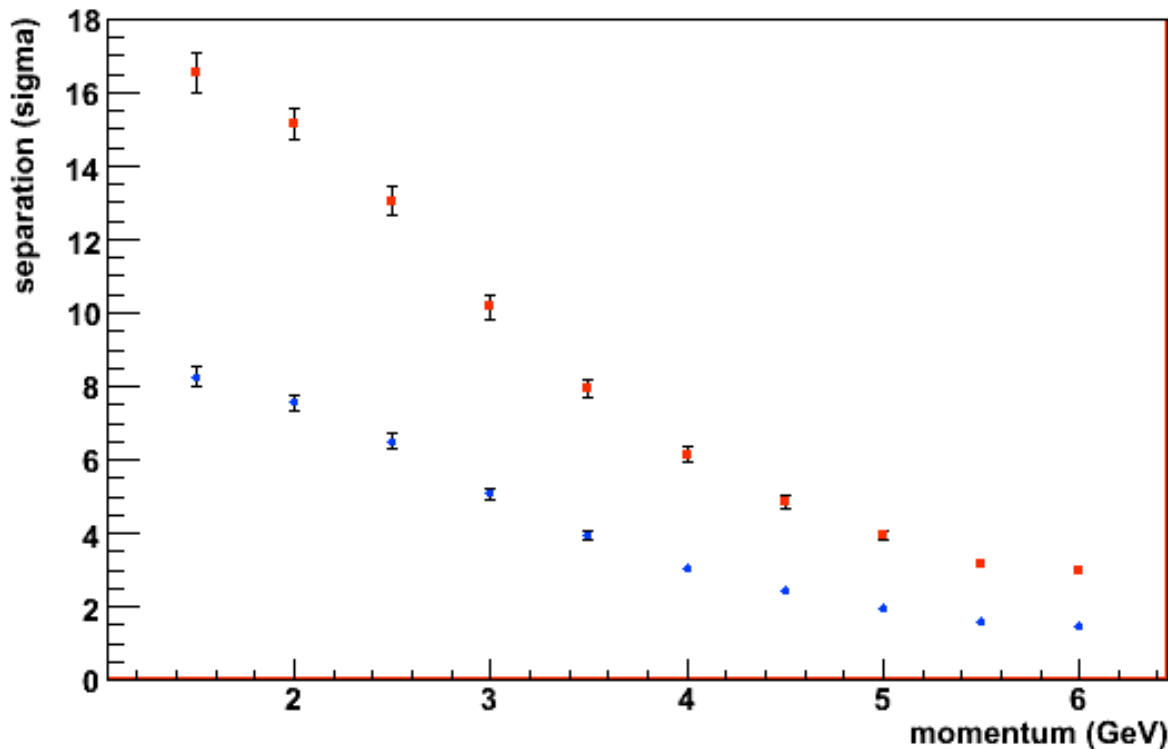


*Fig. 13* The pion-kaon separation vs. momentum using the two different definitions of the  $\sigma$ -separation power.

## Conclusions

Using the fitting method demonstrated in this chapter a clear separation of 4  $\sigma$  is possible up to a pion/kaon momentum of 5 GeV/c. This separation is based on relative time differences of the detected Cherenkov photons and does not require an absolute time measurement by a separate detector.

## References

- [1] M. Düren, M. Ehrenfried, R. Schmidt, J. Streit-Lehmann, *Conceptual Design of a Multi-Chromatic Time-of-Propagation Endcap DIRC for PANDA*, PANDA Internal Report, June 2006,  
<http://www.physik.uni-giessen.de/dueren/giessendirc.pdf>
- [2] R. Schmidt, *Computer Simulation of a Disk DIRC Cherenkov Detector for PANDA*, Diploma Thesis, Justus-Liebig-Universität Giessen, September 2006
- [3] L. Schmitt, private communication, PANDA Cherenkov Workshop at Erlangen (May 16<sup>th</sup> – 17<sup>th</sup>, 2007) and Cherenkov Offline VRVS Meeting, May 23<sup>rd</sup>, 2007